Hindawi
Advances in Polymer Technology
Volume 2019, Article ID 8687450, 11 pages
https://doi.org/10.1155/2019/8687450

Research Article

Thermal Performances of UHMWPE/BN Composites Obtained from Different Blending Methods

Yiyou Guo,[1] Changlin Cao,[1,2] Huibin Cheng,[1] Qinghua Chen,[1,3] Baoquan Huang ,[1] Fubin Luo,[1] and Qingrong Qian ,[1]

[1]*Engineering Research Center of Polymer Green Recycling of Ministry Education and Fujian Key Laboratory of Pollution Control & Resource Reuse, College of Environmental Science and Engineering, Fujian Normal University, Fuzhou 350007, China*
[2]*Key Laboratory for Polymeric Composite and Functional Materials of Ministry of Education and Key Laboratory of High Performance Polymer-Based Composites of Guangdong Province, School of Chemistry, Sun Yat-Sen University, Guangzhou 510275, China*
[3]*Fujian Normal University Fuqing Branch, Fuzhou 350300, China*

Correspondence should be addressed to Baoquan Huang; qbh811@sina.com and Qingrong Qian; qrqian@fjnu.edu.cn

Received 29 May 2019; Accepted 14 August 2019; Published 20 December 2019

Guest Editor: Ming Wang

UHMWPE/BN composites were prepared by solvent mixing (SM) in this work, then were characterized by scanning electron microscope (SEM), Raman mapping, differential scanning calorimeter (DSC), thermogravimetric analysis (TG), and thermal conductivity meter to study the morphology, filler distribution, segregated structure, and thermal stability as well as thermal conductivity. Compared to the traditional melt mixing (MM), SM followed by molding contributes to the construction of segregated structures in UHMWPE composite. This segregated structure can greatly improve the thermal conductivity of the composites. The segregated structure of composites prepared by MM is destroyed by shearing. Moreover, the thermal stability of composites by SM is improved with the increment of BN content, which is better than that of samples by MM, probably resulting from the barrier function of the segregated structure.

1. Introduction

Ultra high molecular weight polyethylene (UHMWPE) is an engineering plastic that is widely used in aerospace, defense military, biological joints, pipeline transportation, etc., due to its outstanding wear resistance, excellent impact resistance, as well as good biocompatibility [1]. A crucial issue currently remaining unresolved is low heat distortion temperature and poor thermal conductivity of UHMWPE, causing UHMWPE to be locally susceptible to thermal deformation, resulting in limited application areas. At present, some researchers manipulate the polymer chain alignment to form orientations [2–4] and the high crystallinity [5, 6] in the matrix to get high thermal conductivity of UHMWPE. There is such a problem that this method requires high production equipment and leads to limited application. In addition to adjust the alignment of polymer chains, UHMWPE doped with the thermally conductive fillers has also gained significant attention. The improved thermal conductivity of UHMWPE composites have been obtained through doping of fillers, such as aluminium nitride (AlN) [7, 8], boron nitride (BN) [9], silicon nitride (Si_3N_4) [10], silicon carbide (SiC) [11], and aluminium oxide [12].

However, UHMWPE cannot be extruded and injection molded like other thermoplastic materials at temperatures above its melting temperature due to its extremely high melt viscosity. Nowadays, the processing of this material is basically limited to compression molding [13–15] and ram extrusion. Therefore, the distribution of thermally conductive fillers in the matrix of UHMWPE has become a key factor affecting the thermal conductivity of composites. In order to allow the thermally conductive particles to be well distributed in the UHMWPE matrix, scholars are currently mixing them: (1) by dispersing the filler and UHMWPE particles in an organic solvent, then volatilizing the organic solvent to dry; (2) by stirring the filler with UHMWPE pellets at high speed in a high speed mixer for a period of time [16]; (3) by mixing the filler and UHMWPE pellets at a certain temperature [17]. For the first type of dispersion, the organic solvents commonly used by research scholars are acetone [18], ethanol [19–22], 1,2 dicholorobenzene [23], etc. Whether dispersed in a solvent

or stirred in a high-mixer, the composite has a segregated structure with a good thermal path, since compression molding is a static flow field. When the filler and the UHMWPE matrix are mixed in a molten state, the segregated structure is damaged to some extent. It has been reported [24] that the order of increase in thermal conductivity is melt mixing, twin roll mixing, solution mixing, and powder mixing. Then, the influence of mixing methods on morphological structure and thermal conductivity, and the relationship between them remains to be further understood.

In this work, the UHMWPE/BN composites were pretreated by MM and SM, and then was performed compression molding. We investigated the effects of microstructure of composites prepared by these two mixing methods on thermal conductivity. Furthermore we focus on the relationship between morphological structure and thermal stability of the composite.

2. Materials and Methods

2.1. Materials. UHMWPE particles with an average diameter of ~150 μm (Mv = 2.5×10^6 g/mol) was purchased from LianLe Chemical Co., Ltd., (Shanghai, China). Hexagonal Boron Nitride platelets with an average diameter of 3 μm and density of 2.25 g/cm^3 were supplied by Yingkou Tianyuan Chemical Research Institute Co. Ltd., (Liaoning, China).

2.2. Preparation of the UHMWPE/BN Composites

2.2.1. Preparation of the UHMWPE/BN Composites by Solvent Mixing. A specified amount (0, 10, 20, 30, 40 wt%) of BN microsheets was fed into ethanol to form a suspension under magnetic stirring for 1 h. Then UHMWPE particles were added into the suspension followed by magnetic stirring at 60°C for another several hours to ensure ethanol completely evaporated. Subsequently, the mixtures were compression-molded at 220°C and 17.6 MPa for 5 min after preheating for 20 min. The resulting UHMWPE/BN composites were cooled to room temperature by cold compression molding for 40 min.

2.2.2. Preparation of the UHMWPE/BN Composites by Melt Mixing. BN microsheets were first dried in an oven at 80°C for 12 h. UHMWPE powder was then mixed with 0, 10, 20, 30, 40wt% of BN microsheets in Harper torque rheometer at 190°C and 30 rpm for 10 min. Then, the mixtures were immediately transferred to a mold for hot pressing at 220°C and 17.6 MPa for another 10 min followed by cold compression molding for 40 min.

2.3. Characterization. The morphology of the samples was obtained with a scanning electron microscope (SEM, JSM-7500F, JEOL, Japan). It was performed at an acceleration voltage of 5 kV. The fractured surfaces of samples were sprayed with Au before SEM examination.

Raman mapping was performed by a micro-laser confocal Raman spectrometer (Thermo Scientific DXR2xi, America). For each sample, a total of 3721 spectra were collected in 70 min on a sample area of 300 × 300 μm with a spatial resolution of 5 μm between spectra. The test condition was that the laser power is 10 mW, and the total exposure is 20 times with 0.025 s exposure time for each spectrum. Peak area of Raman characteristic peak of BN at 1365 cm^{-1} in Raman mapping data was processed by OMMIC analysis software, which can represent the content of BN. In addition, the color in the mapping from dark blue to red indicates the distribution of the BN characteristic peak area from small to large.

Crystalline properties were measured by differential scanning calorimeter (DSC, Q20, TA). The samples were first heated up to 200°C and held isotherm at 200°C for 3 min to remove heat history and then cooled to 40°C. The samples were reheated from 40 to 200°C at 10°C/min. The crystallinity (X_c) was counted according to the following equation:

$$X_c = \frac{\Delta H_m}{\Delta H_{m0} * (1 - \phi)} \times 100\%, \quad (1)$$

where ΔH_m is the melting enthalpy of samples, ΔH_{m0} is the standard enthalpy of PE (290 J/g) [25], and φ is the mass fraction of h-BN platelets.

The weight loss of samples was evaluated by thermal gravimetric analyzer (TGA, Q50, TA) with range from 40 to 600°C at a heating rate of 10°C/min under nitrogen atmosphere.

The thermal conductivity was investigated by a hot–wire thermal conductivity instrument (Xiatech TC3000E, China) according to ASTM D5930. Before thermal conductivity measurement, the hot wire was placed between two same samples of 1 mm thickness with a specific weight on top of the stacked samples to make good contact with samples due to its mechanical flexibility.

3. Results and Discussion

3.1. Morphology of UHMWPE/BN Composites. Figures 1(a) and 1(c) depicts the surface morphologies of UHMWPE nascent powder before and after SM. UHMWPE nascent powder is composed of a plurality of secondary particles connected by fibers. There is no significant changes in morphology of UHMWPE particles after SM. In contrast, the fibers on the surface of UHMWPE particles by MM are melted due to the high temperature. The morphologies of the core-shell UHMWPE/BN particles with 40 wt% BN through two mixing methods are shown in Figures 1(d) and 1(f). It can be seen that BN is uniformly attached to the surface of UHMWPE particles by SM due to smooth surface, less defects, and higher aspect ratio of BN (Figure 1(b)). However, BN tightly adheres to the surface of UHMWPE particles by MM.

Figure 2 depicts the SEM observation of the cryo-fracture surface of the UHMWPE/BN composites, giving more details about microstructure differences of composites prepared via two mixing methods. As shown in Figure 2(a), cryo-fracture surface of pure UHMWPE prepared by SM is porous. There are obvious weld marks between UHMWPE particles. This is because UHMWPE particles are only subjected to the vertical direction by hot pressing without force in the horizontal direction, so that molecular chain motion is limited, resulting in obvious weld lines between the particles and the porous brittle

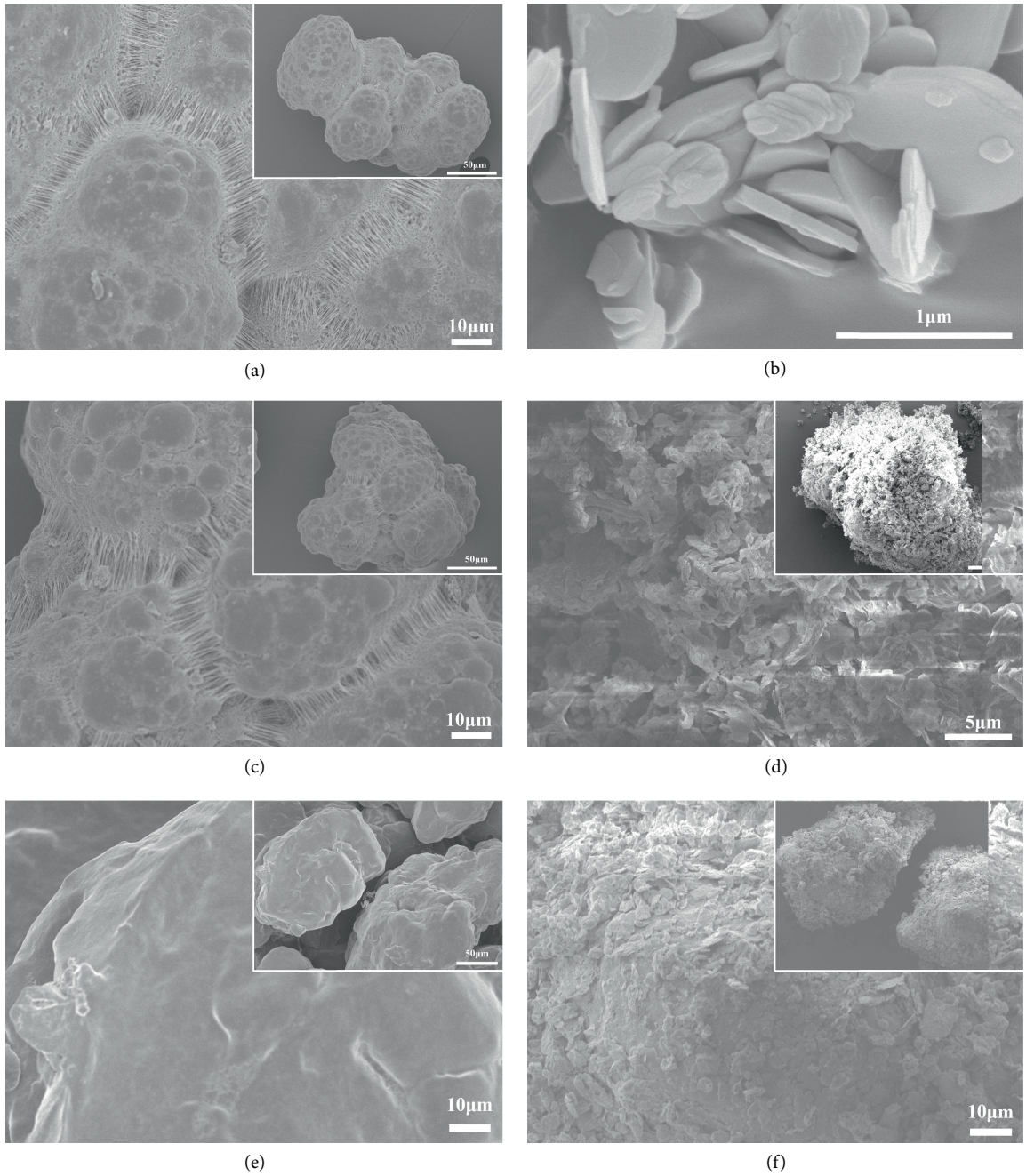

Figure 1: SEM of (a) UMMWPE nascent powder; (b) BN; (c) 0 wt% and (d) 40 wt% BN coated on UHMWPE particles by solvent mixing before hot pressing, (e) 0 wt% and BN (f) 40 wt% BN coated on UHMWPE particles by melt mixing before hot pressing.

profile, while there is no porous brittle profile in cryo-fracture surface of the samples via MM resulting from shear mixing at high temperatures promoting the diffusion of UHMWPE molecular chains inside and between particles. As shown in Figure 4(b), with addition of BN up to 40 wt%, BN adheres to the surface of the UHMWPE particles, and forms BN pathways, which can improve the decomposition hindering effect of the 2D thermal conductivity filler and thermal conductivity of UHMWPE/BN composites. However, it can be seen in Figure 2(d) that part of BN is embedded in UHMWPE particles due to shear at high temperature resulting in damage in segregated structure, which might be the reason why the thermal conductivity and thermal stability of the composite by MM is lower than that of samples via SM.

3.2. Raman Mapping. Raman mapping of UHMWPE/BN composites by SM and MM with various addition of BN is shown in Figure 3. As depicted in Figure 3, Figure a-1, b-1, c-1, d-1, is Raman mapping of test area (Figure a-2, b-2, c-2, d-2) of composites with various addition of BN, respectively. The color in the image from blue to red represents the peak area of Raman characteristic peak of the boron nitride at 1365 cm^{-1} in the composite material from small to large, which can indicate the distribution of BN in the composite matrix.

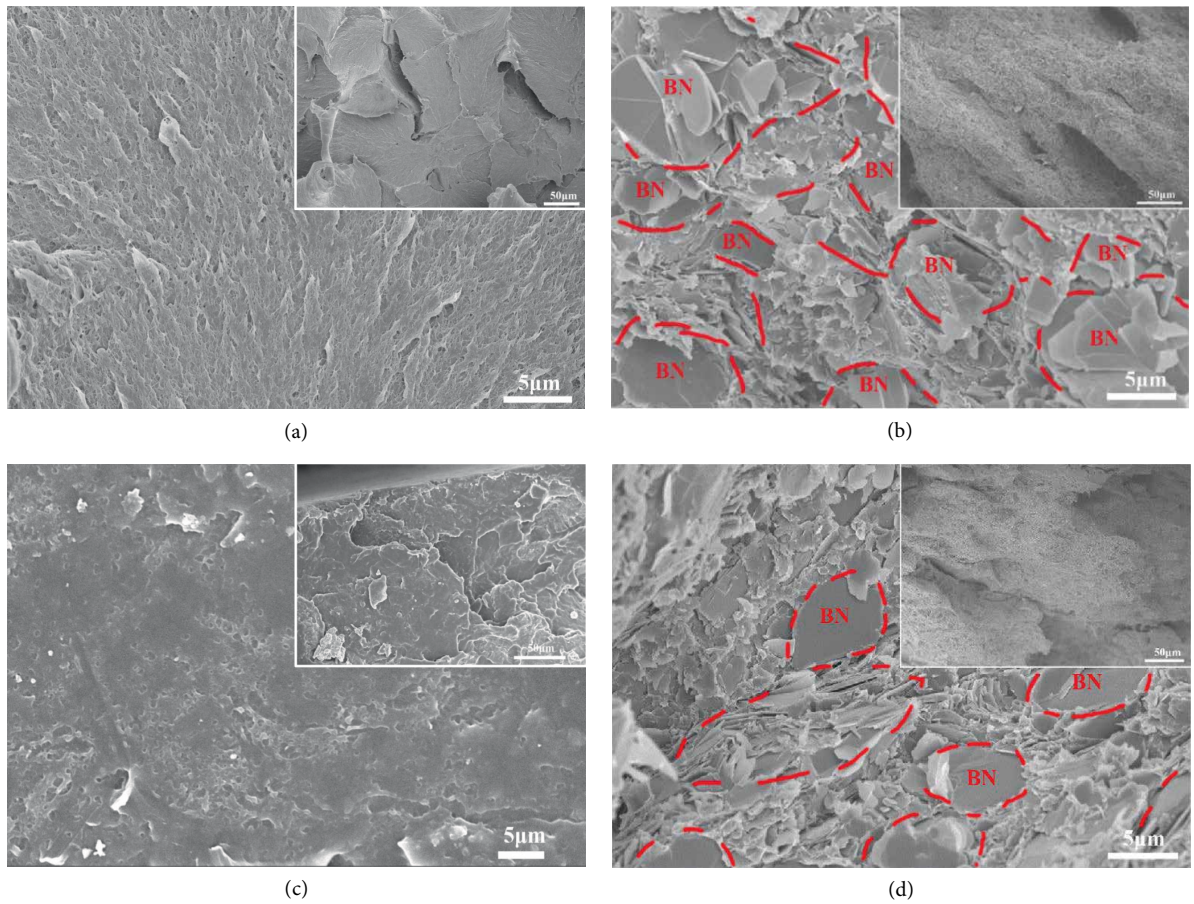

FIGURE 2: SEM of UHMPWE/BN composites by solvent mixing (a) 0 wt% BN; (b) 40 wt% BN; and melt mixing. (c) 0 wt% BN; (d) 40 wt% BN.

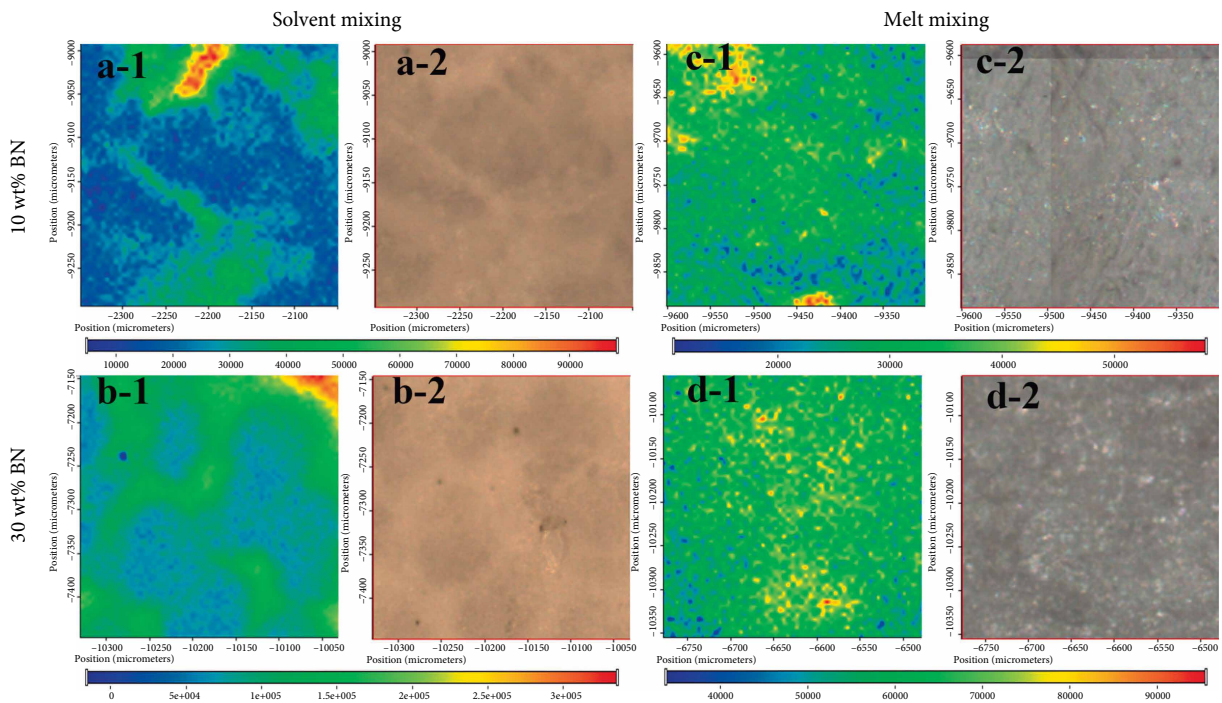

FIGURE 3: Raman Mapping of UHMWPE/BN composites by solvent mixing and melt mixing.

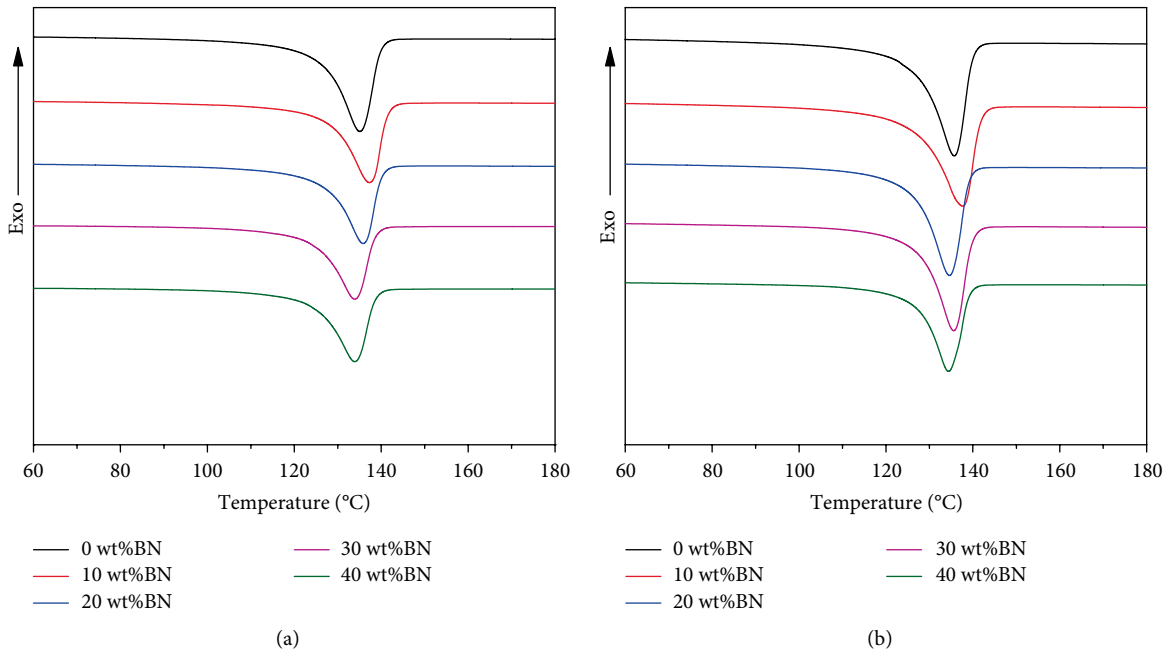

Figure 4: Heating melting function curve of UHMWPE composites by solvent mixing (a) and melt mixing (b), respectively.

Table 1: DSC thermal parameters of UHMWPE/BN composites by solvent mixing and melt mixing.

Mixing method	BN content (wt%)	T_m(°C)	ΔH_m (J/g)	T_c(°C)	ΔH_c (J/g)	X_c(%)
SM	0	135.1	144.3	116.2	148.1	49.8
	10	137.3	131.8	117.4	124.2	50.5
	20	135.9	121.8	117.0	114.4	52.5
	30	133.9	114.0	115.7	107.9	56.2
	40	132.3	106.1	114.4	106.1	61.0
MM	0	135.7	148.6	118.3	145.9	51.2
	10	137.7	145.7	116.6	139.5	55.8
	20	134.6	137.6	117.4	127.7	59.3
	30	135.6	127.1	117.3	119.0	62.6
	40	136.0	108.5	116.9	108.2	62.4

With the increment of BN content, BN coated on the surface of UHMWPE particles forms a continuous thermal conduction path inside the solvent-mixed composite, while the BN signal distribution is relatively uniform in the Raman mapping of composites by MM, indicating that the segregated structure of the composites is damaged due to shearing.

3.3. Crystallization Behavior of UHMWPE/BN Composites. Figure 4 depicts the on-heating DSC curves of UHMWPE composites by different mixing methods and DSC thermal parameters are shown in Table 1. As shown in Table 1, the crystallinity of pure UHMWPE pre-treated by SM and MM is 49.8 and 51.2%, respectively. With the content of BN up to 40 wt%, the crystallinity of the composites via SM and MM increases to 61.0 and 61.4% respectively, due to BN as heterogeneous nucleating agent. However the crystallinity of the composites by MM is higher than that of the samples through SM, resulting from shear promoting better dispersion of BN in the matrix, leading to better heterogeneous nucleation.

3.4. Thermal Stability of UHMWPE/BN Composites. Thermogravimetric analysis (TGA) is carried out to characterize the thermal stability of the composites by different mixing methods under nitrogen atmosphere. The TGA curves and DTA curves are shown in Figure 5 and relevant thermal data are summarized in Table 2. Figure 5 shows that there is only a single stage from the temperature of 400 to 500°C during the thermal decomposition of UHMWPE/BN composites. It illustrates that the addition of BN and different mixing methods does not affect the thermal decomposition behavior. The temperatures at 5%, 30%, and 50% weight loss (T_5, T_{30}, and T_{50}) are shown in Table 2. As Table 2 shows, T_5 of samples by MM decreases with addition of BN and T_{30} and T_{50} has not changed significantly, while T_5, T_{30}, T_{50} of composites by SM both increase. In addition, heat resistance index (HRI) [26] calculated by T_5 and T_{30} of composites by MM decreases slightly from 299.1 to 226°C, while HRI of samples via SM increases from 225 to 230.5°C.

To obtain a better understanding of the thermal stability of the composites by different mixing methods, integral procedural decomposition temperature (IPDT) based on Doyle's proposition [27] and activation energy (E_a) can be used to assess material's thermal stability. The IPDT is determined from TGA curves and reckoned by following equations [28–30]:

$$IPDT(^{\circ}C) = AK \cdot \left(T_f - T_i\right) + T_i, \tag{2}$$

$$A = \frac{S_1 + S_2}{S_1 + S_2 + S_3}, \tag{3}$$

Table 2: Thermal data of UHMWPE/BN composites from TG analyses.

Mixing method	BN content (wt%)	Weight loss temperature(°C)			Heat-resistance index*(°C)	Residual weight/%	
		T_5	T_{30}	T_{50}		Theory	Actual
MM	0	456.5	474.9	480.1	229.1	0	0.20
	10	455.1	475.5	482.3	229.0	10	10.02
	20	451.4	474.3	482.0	227.9	20	20.29
	30	448.8	473.6	482.7	227.2	30	30.23
	40	444.3	472.5	482.7	226.0	40	39.79
SM	0	443.6	469.6	477.0	225.0	0	0.31
	10	436.7	465.3	474.4	222.4	10	10.04
	20	450.6	475.0	482.9	228.0	20	20.67
	30	453.7	476.6	484.7	229.0	30	28.45
	40	457.4	480.1	489.7	230.8	40	40.96

*$T_{\text{Heat-resistance index}} = 0.49 * [T_5 + 0.6(T_{30} - T_5)]$. T_5 and T_{30} is corresponding decomposition temperature of 5 and 30% weight loss, repectively.

$$K = \frac{S_1 + S_2}{S_1}, \tag{4}$$

where A is the area ratio of total experimental curve divided by total TGA curve; K is the coefficient of A (Figure S2); T_i is the onset experimental temperature (50°C, in this work) and T_f is the terminal experimental temperature(550°C). The results of composites by different mixing methods are present in Table 3. The IPDT can be usually attributed to the unstable parts in composites, indicating that the higher IPDT is, the better the thermal stability of composites is.

The E_a required for thermal decomposition of the UHMWPE/BN composites can be reckoned by the Horowitz–Metzger integral kinetic method according to Equation (5) [31–33].

$$\ln\left(\ln(1-\alpha)^{-1}\right) = \frac{E_a}{RT_{\max}^2}\theta, \tag{5}$$

where α is the mass fraction of sample decomposed; the E_a values of the UHMWPE/BN composites can be calculated from the slope of the plot of $\ln\left(\ln(1-\alpha)^{-1}\right)$ versus θ as shown in Figure 6 (kJ/mol); R is the real gas constant (8.314 J/(mol·K)); $T_{\max}$ is decomposition temperature at the maximum weight loss rate (°C); θ is the difference between decomposition temperature T and $T_{\max}(K)$.

E_a is a parameter used to evaluate the thermal stability of materials. The higher E_a value the polymer composites have, the more thermally stable it is. Generally, relatively large crosslinking density results in high decomposition temperature [29]. It can be seen in Figures S1, S3, and Table S1 that both IPDT and the E_a rise with the increase of relative molecular weight of UHMWPE, indicating that the higher relative molecular mass UHMWPE has, the higher the internal physical entanglement density is and the better thermal stability UHMWPE has [34, 35]. The IPDT and E_a of UHMWPE with the same relative molecular mass prepared by MM is 499.7°C and 530.27 kJ/mol, respectively higher than the IPDT and the E_a of UHMWPE prepared by SM, which is 475.5°C and 478.65 kJ/mol. During the MM process, the shearing action leads to a certain decrease in the relative molecular mass of UHMWPE, but also promotes the increase in physical entanglement density, resulting in better thermal stability.

As shown in Table 3, with addition of BN, the IPDT of the composites increases gradually and the IPDT of the melt-mixed samples is higher than that of the solvent-mixed samples, indicating that MM increases the inherent thermal stability of the composites. In addition, with the increment of BN content, the E_a values of composites via MM or SM are reduced compared to pure UHMWPE resulting from the introduction of high thermal conductivity filler BN causing heat to pass faster in the composites. And the E_a values of composites by MM decrease more than those of samples via SM. This is because that the segregated structure of the composites through SM makes the 2D material BN hinder the diffusion of the volatile decomposition part [36], while the segregated structure of samples via MM is damaged to some extent due to shear at high temperature. Thereby, the contribution of both IPDT and E_a induces differences in thermal stability between samples prepared by MM and SM [37].

3.5. Thermal Conductivities of the UHMWPE/BN Composites. Figure 7 illustrates the thermal conductivity and enhancement ratio of the UHMWPE/BN composites by different mixing methods. The thermal conductivity enhancement ratio is defined as:

$$X = \frac{\lambda_c - \lambda_p}{\lambda_p} * 100\%, \tag{6}$$

where X is the thermal conductivity enhancement ratio; λ_c is the thermal conductivity of the composite; λ_p is the thermal conductivity of pure UHMWPE. As shown in Figure 7(a), it can be seen that the thermal conductivity of two mixing methods is increasing with the increment of BN content. The thermal conductivity of composites prepared through MM increases from 0.38 to 1.50 $\text{Wm}^{-1}\text{K}^{-1}$, increased by 294.74% with addition of BN up to 40 wt%, while the thermal conductivity of composites prepared by SM is up to 1.76 $\text{Wm}^{-1}\text{K}^{-1}$, increased by 363.16% at the same filler content. It is obviously seen that the thermal conductivity of composites prepared by

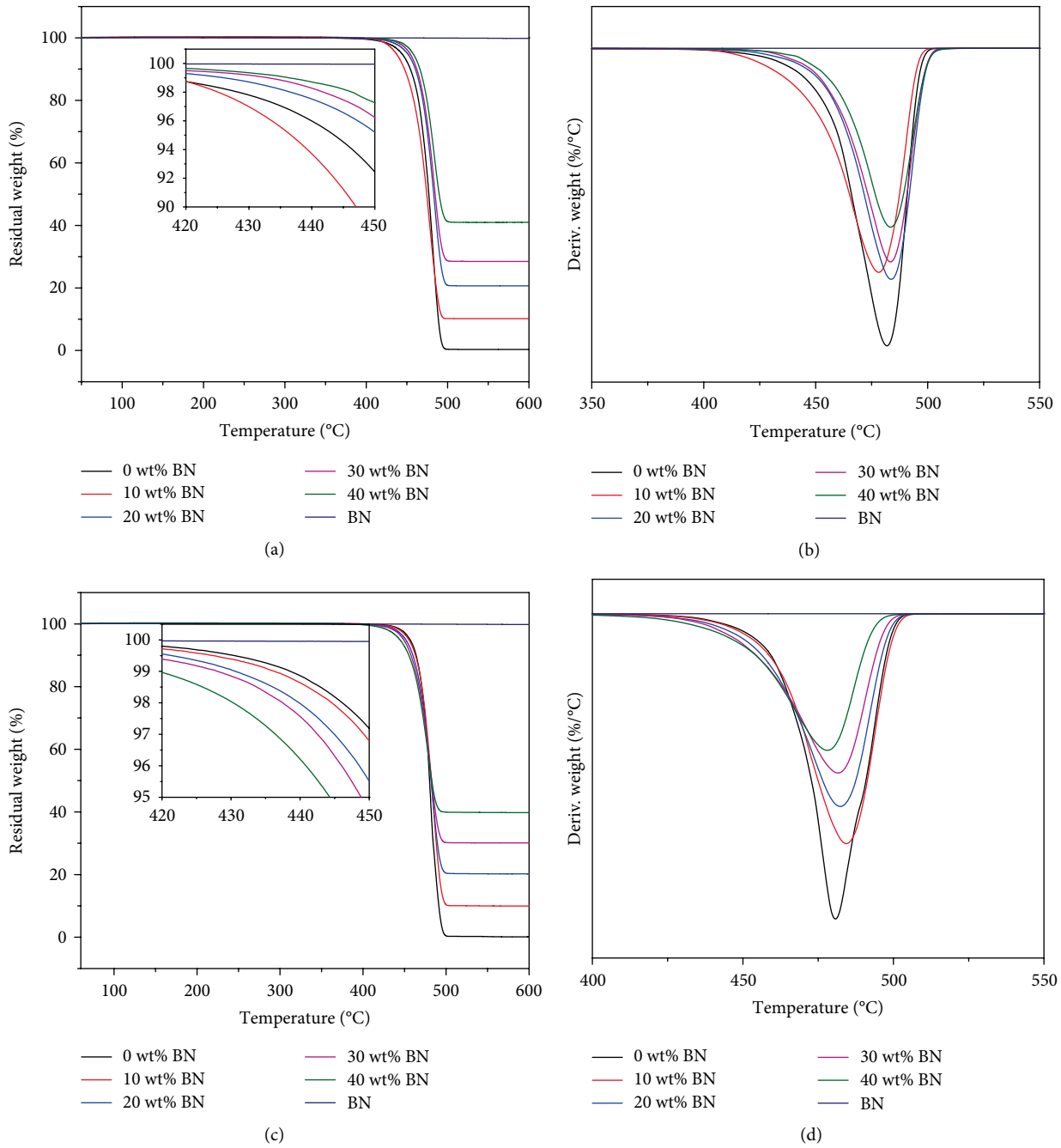

Figure 5: TGA and DTA curves of UHMWPE/BN composites by solvent mixing (a) (b) and melt mixing (c) (d).

Table 3: Thermal stabilities of the composites by different mixing obtained from TGA curves.

BN content (wt%)	T_{max} [a] (°C)		IPDT (°C)		E_a [b] (kJ/mol)	R^2	E_a [b] (kJ/mol)	R^2
	SM	MM	SM	MM	SM		MM	
0	481.8	480.8	475.5	499.7	478.65	0.997	530.27	0.997
10	478.2	484.4	534.8	566.7	335.62	0.999	430.27	0.995
20	483.7	482.4	535.7	649.6	356.59	0.991	356.34	0.991
30	483.4	481.6	626.4	742.9	342.05	0.986	305.78	0.986
40	483.5	478.1	705.9	875.2	333.03	0.979	281.07	0.982

[a]The decomposition temperature at the maximum rate of the weight loss. [b]The activation energy calculate by Horowitz–Metzger integral kinetic method.

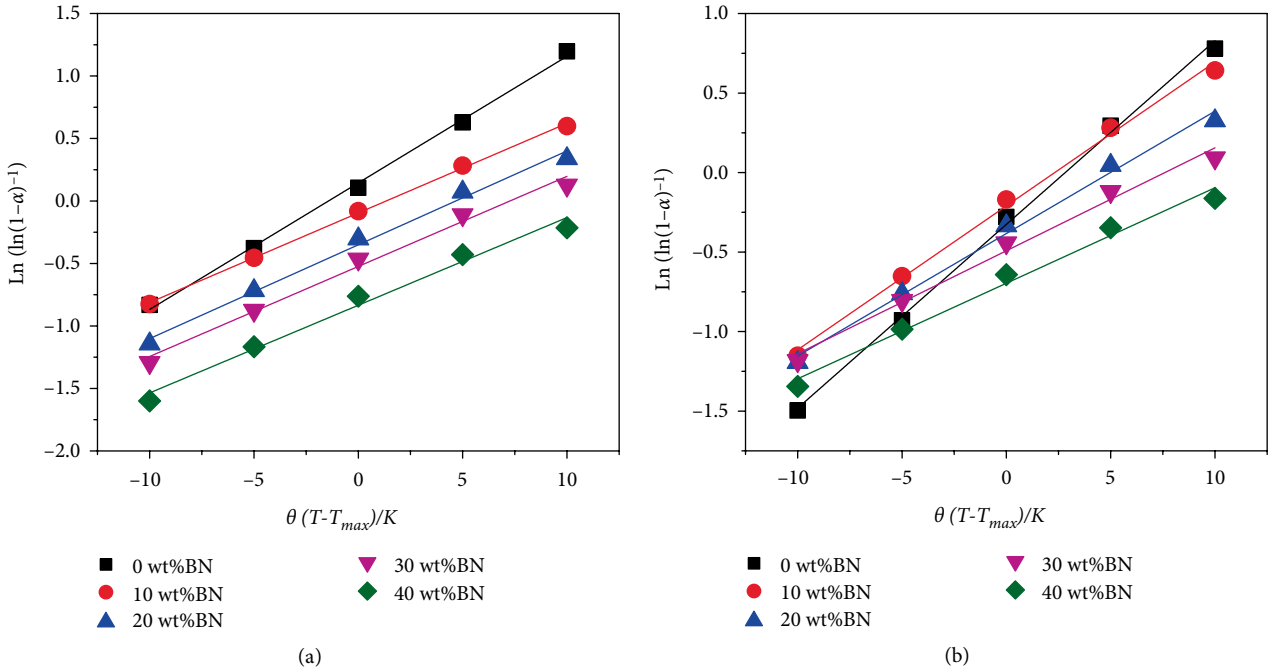

FIGURE 6: The plots of $\ln\left(\ln(1-\alpha)^{-1}\right)$ versus θ as shown for the UHMWPE/BN composites by solvent mixing (a) and melt mixing (b).

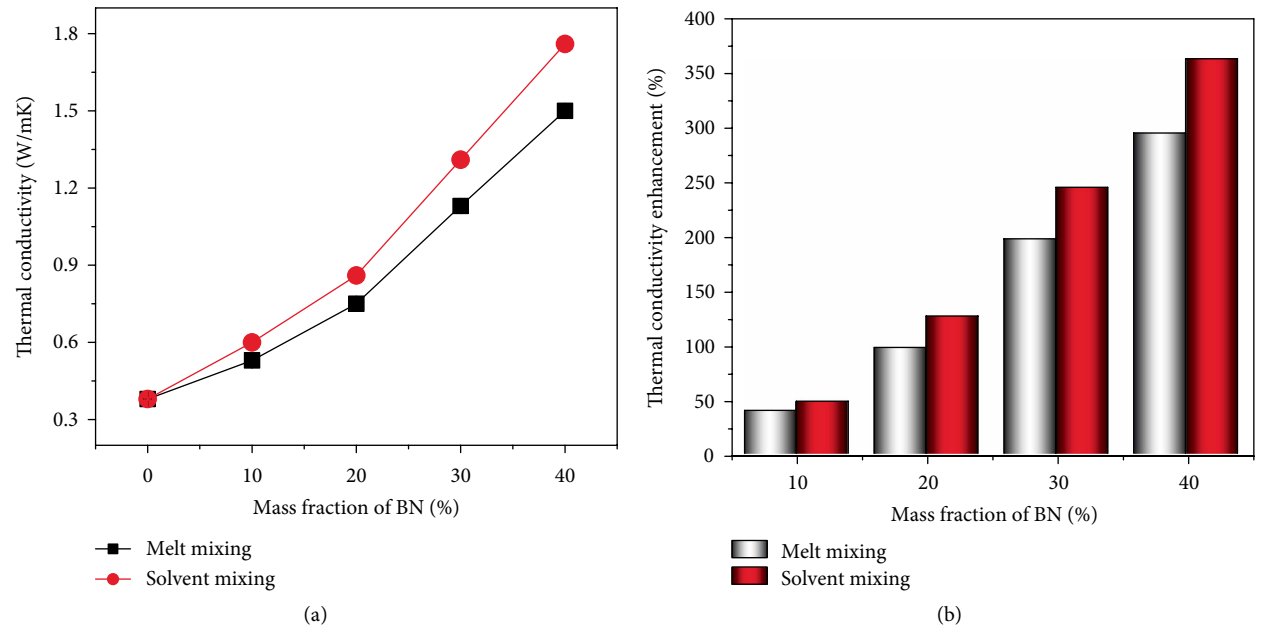

FIGURE 7: Thermal conductivity and enhencement of the UHMWPE/BN composites by melt mixing and solvent mixing.

SM is superior to that of composites prepared by MM, which is consistent with the results of some researchers [38–40]. SM helps BN to physically adhere to the surface of UHMWPE particles, and composite materials with isolated structure can be prepared by molding, which results in improvement of thermal conductivity of UHMWPE/BN composites. However, the isolated structure of the composite is destroyed after the MM, which causes the thermal path inside the UHMWPE to be destroyed, resulting in lower thermal conductivity than that of composites by SM.

The effective thermal conductivities of two-phase polymeric composites have been predicted by many researchers via proposing theoretical and empirical models. Hereon, Agari's semi-empirical model [41–45] can fit better results than other models. The logarithmic equation of Agari is shown as follows:

$$\log\lambda = VC_2\log\lambda_2 + (1-v)\log(\lambda_1 C_1), \tag{7}$$

where C_1 denotes the effect of doping BN on the UHMWPE structure; C_2 denotes the contribution of BN to construction

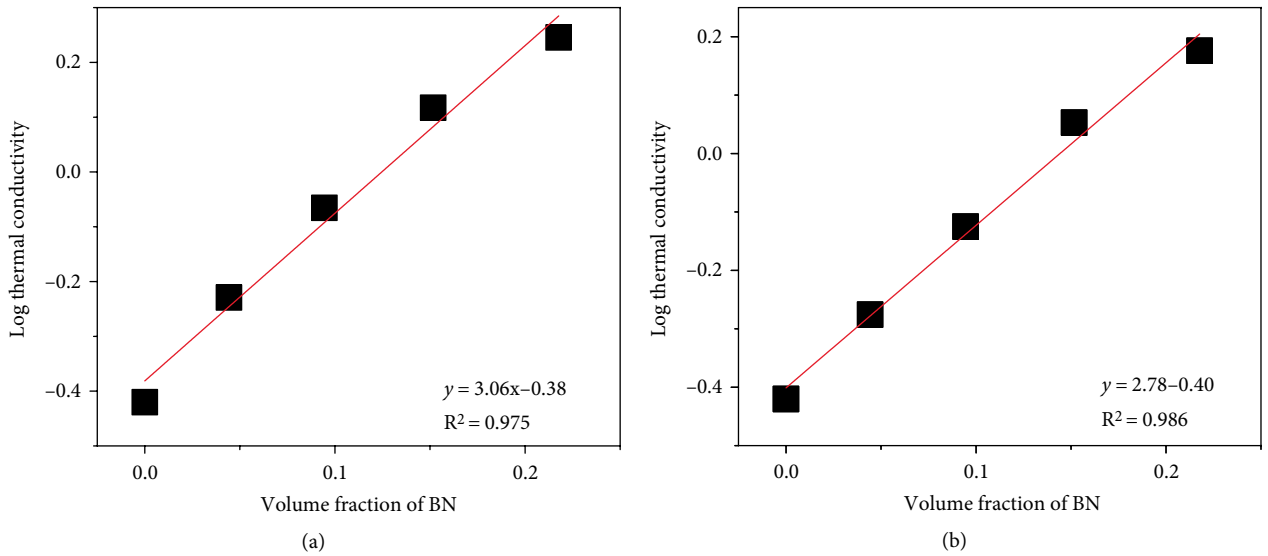

Figure 8: Logarithmic thermal conductivities of the UHMWPE composites as a function of the BN volume fraction by solvent mixing (a) and melt mixing (b).

of continuous thermally conductive chains & networks, $0 < C_2 < 1$, the easier formation of thermal conduction paths of fillers, the more the C_2 close to 1; V denotes the volume fraction of fillers; λ, λ_2, and λ_1 denote the thermal conductivity of composites, fillers and polymeric matrix, respectively.

Figure 8 shows the logarithmic values of thermal conductivities as a function of the BN volume fraction by MM and SM. Herein, λ_2 is 290 $Wm^{-1}K^{-1}$ and λ_1 is 0.38 $Wm^{-1}K^{-1}$, According to Equation (7), the results are calculated in Table S2. It can be seen that the parameters of C_2 of composites by SM is higher than that of samples by MM, revealing that SM makes it easier for BN to form continuous thermally conductive networks in the UHMWPE matrix than MM, resulting in better thermal conductivity of the composite.

4. Conclusions

UHMWPE/BN composites, which were prepared by SM and MM, were characterized through SEM, Raman mapping, TG, DSC, and thermal conductivity meter. It aims to mainly discuss the effect of different mixing methods on the thermal conductivity and thermal stability of the composites. The samples by SM have a better segregated structure than the samples by MM whose segregated structure is destroyed due to high temperature shearing. Although the crystallinity of samples via MM is larger than that of the SM, the thermal conductivity of composites by SM is better than that of samples by MM, resulting from structural differences caused by the difference between the two mixing methods. The reason is explained by calculated IPDT and activation energy of the composites that the thermal stability of the composite by SM increases with continuous addition of BN due to the decomposition hindering effect of the 2D thermal conductivity filler, while the thermal stability of the composite by MM decreases.

Data Availability

The data used to support the findings of this study are available from the corresponding author upon request.

Conflicts of Interest

The authors declare that they have no conflicts of interest.

Funding

Financial supports from the National Key Research and Development Program of China (2016YFB0302300).

Acknowledgments

This research was supported by the Engineering Research Center of Polymer Green Recycling of Ministry Education and Fujian Key Laboratory of Pollution Control & Resource Reuse, College of Environmental Science and Engineering Fujian Normal University. The authors are grateful to Xianning Wang for the guidance and maintenance of the polymer processing equipment.

Supplementary Materials

Figure S1: TGA curves of UHMWPE particles with various relative molecular weight. Table S1: thermal data of UHMWPE nascent powder with different relative molecular weight. Figure S2: Schematic representation of S1, S2, and S3 for A and K. Figure S3: the plots of $\ln\left(\ln(1-\alpha)^{-1}\right)$ versus θ as shown for the UHMWPE with various relative molecular weights. Table S2: thermal data of UHMWPE nascent powder with different relative molecular weight. (*Supplementary Materials*)

References

[1] S. M. Kurtz, *The UHMWPE Handbook: Ultra-high Molecular Weight Polyethylene in Total Joint Replacement*, Elsevier, Amsterdam, The Netherlands, 2004.

[2] W. Zhou, C. Wang, T. Ai, K. Wu, F. Zhao, and H. Gu, "A novel fiber-reinforced polyethylene composite with added silicon nitride particles for enhanced thermal conductivity," *Composites Part A: Applied Science and Manufacturing*, vol. 40, no. 6–7, pp. 830–836, 2009.

[3] C. L. Choy, Y. Fei, and T. G. Xi, "Thermal conductivity of gel-spun polyethylene fibers," *Journal of Polymer Science Part B: Polymer Physics*, vol. 31, no. 3, pp. 365–370, 1993.

[4] S. Ronca, T. Igarashi, G. Forte, and S. Rastogi, "Metallic-like thermal conductivity in a lightweight insulator: solid-state processed ultra high molecular weight polyethylene tapes and films," *Polymer*, vol. 123, pp. 203–210, 2017.

[5] Y. Guo and S. N. Leung, "Strain-induced oriented crystallization of UHMWPE: enhanced thermal conductivity through molecular chain alignment," *AIP Advances*, vol. 8, no. 4, p. 045126, 2018.

[6] F. Zhong, R. Thomann, and R. Mülhaupt, "Processing–nanostructure–property relationships of all-polyethylene composites reinforced by flow-induced oriented crystallization of UHMWPE," *Macromolecular Materials and Engineering*, vol. 303, no. 5, p. 1800022, 2018.

[7] Y. Wang, X. Qiao, J. Wan, Y. Xiao, and X. Fan, "Preparation of AlN microspheres/UHMWPE composites for insulating thermal conductors," *RSC Advances*, vol. 6, no. 83, pp. 80262–80267, 2016.

[8] W. Zhou, "Thermal and dielectric properties of the AlN particles reinforced linear low-density polyethylene composites," *Thermochimica Acta*, vol. 512, no. 1–2, pp. 183–188, 2011.

[9] C. Gao, H. Lu, H. Ni, and J. Chen, "Structure, thermal conductive, dielectric and electrical insulating properties of UHMWPE/BN composites with a segregated structure," *Journal of Polymer Research*, vol. 25, no. 1, p. 6, 2018.

[10] Q. An, S. Qi, and W. Zhou, "Thermal, electrical, and mechanical properties of Si3N4 filled LLDPE composite," *Polymer Composites*, vol. 30, no. 7, pp. 866–871, 2009.

[11] J. Gu, Y. Guo, Z. Lv, W. Geng, and Q. Zhang, "Highly thermally conductive POSS-g-SiCp/UHMWPE composites with excellent dielectric properties and thermal stabilities," *Composites Part A: Applied Science and Manufacturing*, vol. 78, pp. 95–101, 2015.

[12] S. Yang, W. Li, S. Bai, and Q. Wang, "Fabrication of morphologically controlled composites with high thermal conductivity and dielectric performance from aluminum nanoflake and recycled plastic package," *ACS Applied Materials & Interfaces*, vol. 11, no. 3, pp. 3388–3399, 2018.

[13] H. Pang, Y. Y. Piao, Y. Q. Tan, G.-Y. Jiang, J.-H. Wang, and Z.-M. Li, "Thermoelectric behaviour of segregated conductive polymer composites with hybrid fillers of carbon nanotube and bismuth telluride," *Materials Letters*, vol. 107, pp. 150–153, 2013.

[14] L. C. Jia, D. X. Yan, X. Jiang et al., "Synergistic effect of graphite and carbon nanotubes on improved electromagnetic interference shielding performance in segregated composites," *Industrial & Engineering Chemistry Research*, vol. 57, no. 35, pp. 11929–11938, 2018.

[15] S. Zhao, D. Lou, P. Zhan et al., "Heating-induced negative temperature coefficient effect in conductive graphene/polymer ternary nanocomposites with a segregated and double-percolated structure," *Journal of Materials Chemistry C*, vol. 5, no. 32, pp. 8233–8242, 2017.

[16] Z. G. Wang, F. Gong, W. C. Yu et al., "Synergetic enhancement of thermal conductivity by constructing hybrid conductive network in the segregated polymer composites," *Composites Science and Technology*, vol. 162, pp. 7–13, 2018.

[17] Y. F. Huang, J. Z. Xu, J. S. Li, B.-X. He, L. Xu, and Z.-M. Li, "Mechanical properties and biocompatibility of melt processed, self-reinforced ultrahigh molecular weight polyethylene," *Biomaterials*, vol. 35, no. 25, pp. 6687–6697, 2014.

[18] K. Liu, S. Ronca, E. Andablo-Reyes, G. Forte, and S. Rastogi, "Unique rheological response of ultrahigh molecular weight polyethylenes in the presence of reduced graphene oxide," *Macromolecules*, vol. 48, no. 1, pp. 131–139, 2014.

[19] S. K. Reddy, S. Kumar, K. M. Varadarajan, P. R. Marpu, T. K. Gupta, and M. Choosri, "Strain and damage-sensing performance of biocompatible smart CNT/UHMWPE nanocomposites," *Materials Science and Engineering: C*, vol. 92, pp. 957–968, 2018.

[20] Y. Wang, J. Yang, S. Zhou, W. Zhang, and R. Chuan, "Electrical properties of graphene nanoplatelets/ultra-high molecular weight polyethylene composites," *Journal of Materials Science: Materials in Electronics*, vol. 29, no. 1, pp. 91–96, 2018.

[21] C. P. Feng, L. Chen, F. Wei, H. Y. Ni, J. Chen, and W. Yang, "Highly thermally conductive UHMWPE/graphite composites with segregated structures," *RSC Advances*, vol. 6, no. 70, pp. 65709–65713, 2016.

[22] T. K. Gupta, M. Choosri, K. M. Varadarajan, and S. Kumar, "Self-sensing and mechanical performance of CNT/GNP/UHMWPE biocompatible nanocomposites," *Journal of Materials Science*, vol. 53, no. 11, pp. 7939–7952, 2018.

[23] Z. Zhang, S. Mogurampelly, S. Percec et al., "Mechanically strong polymer sheets from aligned ultrahigh-molecular-weight polyethylene nanocomposites," *The Journal of Physical Chemistry Letters*, vol. 9, no. 10, pp. 2652–2658, 2018.

[24] Y. Agari, A. Ueda, and S. Nagai, "Thermal conductivities of composites in several types of dispersion systems," *Journal of Applied Polymer Science*, vol. 42, no. 6, pp. 1665–1669, 1991.

[25] F. J. Medel, M. J. Martínez-Morlanes, P. J. Alonso, J. Rubín, F. J. Pascual, and J. A. Puértolas, "Microstructure, thermooxidation and mechanical behavior of a novel highly linear, vitamin E stabilized, UHMWPE," *Materials Science and Engineering: C*, vol. 33, no. 1, pp. 182–188, 2013.

[26] Z. Han and A. Fina, "Thermal conductivity of carbon nanotubes and their polymer nanocomposites: a review," *Progress in Polymer Science*, vol. 36, no. 7, pp. 914–944, 2011.

[27] C. D. Doyle, "Estimating thermal stability of experimental polymers by empirical thermogravimetric analysis," *Analytical Chemistry*, vol. 33, no. 1, pp. 77–79, 1961.

[28] S. J. Park and M. S. Cho, "Thermal stability of carbon-MoSi2-carbon composites by thermogravimetric analysis," *Journal of Materials Science*, vol. 35, no. 14, pp. 3525–3527, 2000.

[29] M. S. Goyat, S. Ray, and P. K. Ghosh, "Innovative application of ultrasonic mixing to produce homogeneously mixed nanoparticulate-epoxy composite of improved physical properties," *Composites Part A: Applied Science and Manufacturing*, vol. 42, no. 10, pp. 1421–1431, 2011.

[30] C. F. Kuan, W. J. Chen, Y. L. Li, C.-H. Chen, H.-C. Kuan, and C.-L. Chiang, "Flame retardance and thermal stability of carbon nanotube epoxy composite prepared from sol–gel method," *Journal of Physics and Chemistry of Solids*, vol. 71, no. 4, pp. 539–543, 2010.

[31] S. Y. Wu, Y. L. Huang, C. C. M. Ma, S.-M. Yuen, C.-C. Teng, and S.-Y. Yang, "Mechanical, thermal and electrical properties of aluminum nitride/polyetherimide composites," *Composites Part A: Applied Science and Manufacturing*, vol. 42, no. 11, pp. 1573–1583, 2011.

[32] Y. Zhang, X. Ge, F. Deng, M.-C. Li, and U. R. Cho, "Fabrication and characterization of rice bran carbon/styrene butadiene rubber composites fabricated by latex compounding method," *Polymer Composites*, vol. 38, no. 11, pp. 2594–2602, 2017.

[33] K. E. Gonsalves, X. Chen, and M. I. Baraton, "Mechanistic investigation of the preparation of polymer/ceramic nanocomposites," *Nanostructured Materials*, vol. 9, no. 1–8, pp. 181–184, 1997.

[34] X. L. Wang, R. K. Y. Li, Y. X. Cao, and Y. Z. Meng, "Essential work of fracture analysis of poly (propylene carbonate) with varying molecular weight," *Polymer Testing*, vol. 24, no. 6, pp. 699–703, 2005.

[35] A. Mamun, S. M. M. Rahman, S. Roland, and R. Mahmood, "Impact of molecular weight on the thermal stability and the miscibility of poly (ε-caprolactone)/polystyrene binary blends," *Journal of Polymers and the Environment*, vol. 26, no. 8, pp. 3511–3519, 2018.

[36] W. Jin, L. Yuan, G. Liang, and A. Gu, "Multifunctional cyclotriphosphazene/hexagonal boron nitride hybrids and their flame retarding bismaleimide resins with high thermal conductivity and thermal stability," *ACS applied materials & interfaces*, vol. 6, no. 17, pp. 14931–14944, 2014.

[37] Z. Su, H. Wang, X. Ye et al., "Anisotropic thermally conductive flexible polymer composites filled with hexagonal born nitride (h-BN) platelets and ammine carbon nanotubes (CNT-NH2): Effects of the filler distribution and orientation," *Composites Part A: Applied Science and Manufacturing*, vol. 109, pp. 402–412, 2018.

[38] R. Xia, M. Sun, B. Yang et al., "Morphology, Thermal and Crystallization Properties of Polyamide-6/Boron Nitride (BN) Thermal Conductive," *Composites*, vol. 42, no. 2, pp. 230–241, 2018.

[39] Q. Mu and S. Feng, "Thermal conductivity of graphite/silicone rubber prepared by solution intercalation," *Thermochimica Acta*, vol. 462, no. 1–2, pp. 70–75, 2007.

[40] T. Liu, J. Li, X. Wang et al., "Preparation and properties of thermal conductive polyamide 66 composites," *Journal of Thermoplastic Composite Materials*, vol. 28, no. 1, pp. 32–45, 2015.

[41] Y. Agari, A. Ueda, and S. Nagai, "Thermal conductivity of a polymer composite," *Journal of Applied Polymer Science*, vol. 49, no. 9, pp. 1625–1634, 1993.

[42] Y. Agari, A. Ueda, and S. Nagai, "Thermal conductivity of a polyethylene filled with disoriented short-cut carbon fibers," *Journal of Applied Polymer Science*, vol. 43, no. 6, pp. 1117–1124, 1991.

[43] J. Gu, N. Li, L. Tian, Z. Lv, and Q. Zhang, "High thermal conductivity graphite nanoplatelet/UHMWPE nanocomposites," *RSC Advances*, vol. 5, no. 46, pp. 36334–36339, 2015.

[44] S. Yang, S. Bai, W. Duan, and Q. Wang, "Production of Value-Added Composites from Aluminum-Plastic Package Waste via Solid-State Shear Milling Process," *ACS Sustainable Chemistry & Engineering*, vol. 6, no. 3, pp. 4282–4293, 2018.

[45] S. Yang, W. Li, S. Bai, and Q. Wang, "High-performance thermal and electrical conductive composites from multilayer plastic packaging waste and expanded graphite," *Journal of Materials Chemistry C*, vol. 6, no. 41, pp. 11209–11218, 2018.